


Article

A divergent haplotype with a large deletion at the berry color locus causes a white-skinned phenotype in grapevine

Jean-Sébastien Reynard ^{1,*}, Justine Brodard², David Roquis³, Eric Droz², Komlan Avia⁴, Thibaut Verdenal¹, Vivian Zufferey¹, Thierry Lacombe^{5,6}, Daniel Croll⁷ and Jean-Laurent Spring¹

¹Viticulture, Agroscope, Av. de Rochettaz 21, 1009 Pully, Switzerland

²Virology, Agroscope, Route de Duillier 60, 1260 Nyon, Switzerland

³Hepia, Route de Presinge 150, 1254 Jussy, Switzerland

⁴INRAE, Université de Strasbourg, UMR SVQV, 68000 Colmar, France

⁵UMR AGAP Institut, CIRAD, INRAE, Institut Agro, Univ Montpellier, F-34398 Montpellier, France

⁶IFV-INRAE-Institut Agro, UMT Geno-Vigne[®], F-34398 Montpellier, France

⁷Institute of Biology, Laboratory of Evolutionary Genetics, 2000 Neuchâtel, Switzerland

*Corresponding author. E-mail: jean-sebastien.reynard@agroscope.admin.ch

Abstract

The current genetic model explaining berry skin color in *Vitis vinifera* is incomplete and fails to predict berry skin color phenotypes for one allele of *VvMybA1*, referred to as *VvMybA1_SUB*. Our study focuses on this specific allele, revealing that the haplotype containing *VvMybA1_SUB* (haplotype F) represents an ancient lineage of the berry color locus. Within haplotype F, we identified two functional subhaplotypes, HapF1 and HapF2, associated with black-skinned phenotype, and one non-functional subhaplotype, HapF^{DEL}, responsible for white-skinned phenotype. HapF1 likely originated from wild populations domesticated in the Near East and subsequently spread globally with the expansion of viticulture. In contrast, HapF2 has a more restricted distribution and may have emerged from hybridization events between cultivated grapevines and local wild populations as viticulture migrated to the Italian peninsula. Furthermore, we found that in white-skinned berry cultivar, HapF has undergone a large deletion at the berry color locus, removing the majority of the *VvMybA* genes. Previous works suggested a single common origin for white-skinned varieties during grapevine domestication. Our results challenge this notion, instead proposing that white-skinned grape cultivars arose at least twice during grapevine domestication history. Alongside the major haplotype A, some white-skinned cultivars, such as cv. ‘Sultanina’ harbor HapF^{DEL}. Since HapF^{DEL} is present only in table grape varieties, we suggest that it likely arose from a recent mutational event and dispersed along the ancient Silk Road into East Asia. These findings enhance our understanding of the genetic diversity and evolutionary trajectory of grapevine cultivars, offering insights into their domestication and spread across different geographical regions.

Introduction

Since the seminal work of Gregor Mendel (1822–1884) in the middle of the 19th century, the inheritance and genetic bases of color variation in plants have attracted significant scientific interest. The red, purple, and blue coloration of plant tissues is mainly caused by a class of pigments called anthocyanins. These secondary metabolites are stored in plant vacuoles and belong to the flavonoid class. Their biosynthesis is a branch of the phenylpropanoid pathway, originating from phenylalanine [1]. Anthocyanins are crucial for various plant physiological processes and play a major role in ecological interactions, including those with pollinators and seed dispersers [2]. In Eurasian grapevine (*Vitis vinifera*), anthocyanins begin to accumulate in berry skin at veraison (i.e., the onset of ripening). This accumulation is influenced by both genetic factors and the environment. The presence or absence of anthocyanins in berry skin is crucial for producing wines of various colors. Additionally, berry color is a key

criterion for ampelography (i.e., the description of the different grapevine cultivars), allowing the classification of thousands of different cultivars into two primary categories based on whether anthocyanins are present in the berry skin.

Most of the cultivars grown today are the result of a domestication process from the wild ancestor *Vitis vinifera* subsp. *sylvestris* (hereafter *V. sylvestris*). Since wild grapes are always blue/black at maturity, a trait associated with attracting birds for seed dispersal, the original form of *V. sylvestris* most likely exhibited a black-skinned phenotype [3]. Evidence suggests that white wine was already produced in Egypt during the reign of pharaoh Tutankhamun (1341–1323BCE) [4], although almost all the documents attest to a cultivation of black grapes. White cultivars were already known to be cultivated by ancient civilizations during antiquity, such as the Greeks and Romans.

White grape varieties do not produce anthocyanins in berry skin during the ripening phase. Classic genetic experiments have

Received: 10 October 2024; Accepted: 25 February 2025; Published: 6 March 2025; Corrected and Typeset: 1 June 2025

© The Author(s) 2025. Published by Oxford University Press on behalf of Nanjing Agricultural University. This is an Open Access article distributed under the terms of the Creative Commons Attribution License (<https://creativecommons.org/licenses/by/4.0/>), which permits unrestricted reuse, distribution, and reproduction in any medium, provided the original work is properly cited.

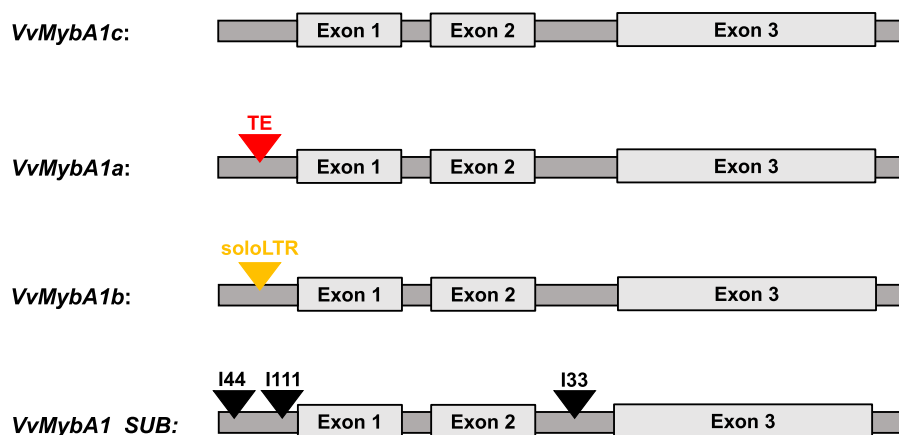


Figure 1. Schematic illustration of different alleles of the *VvMybA1* gene. *VvMybA1c* is the functional allele; *VvMybA1a* is the non-functional white allele containing *Gret1*, a transposable element (TE), in the promoter region of the gene. For *VvMybA1b*, *Gret1* is partially excised, and only a portion (soloLTR) remains in the promoter region. The *VvMybA1_SUB* allele has three small insertions (black triangles: 44 bp, 111 bp, and 33 bp) compared to *VvMybA1c*.

long shown that for *V. vinifera*, berry skin color is controlled by a major locus, and the white-skinned berry allele is recessive [5]. The first work to identify and characterize some genes from the flavonoid pathway in *V. vinifera* was carried out 30 years ago [6]. Shortly after, others have demonstrated that unlike in grape varieties of other colors, *VvUFGT* (UDP-glucose: flavonoid-3-O-glucosyltransferase) expression is absent in white-skinned cultivars [7]. The enzyme UFGT catalyzes the glycosylation of unstable colorless anthocyanidin aglycones into pigmented anthocyanins. *VvUFGT* was later shown to be transcriptionally regulated by MYB factors [8]. The first MYB gene was initially identified as an oncogene in an avian myeloblastosis virus [9], and similar genes were found later in plants. Numerous studies have indicated that the MYB family constitutes one of the largest transcription factors in plants, and some MYB factors have been shown to be involved in the anthocyanin biosynthesis pathway in *Zea mays* [10]. In *V. vinifera*, a region on chromosome 2 has been identified as the major genetic determinant of berry skin coloration and is called the berry color locus (BCL) [11]. This locus was shown to contain multiple copies of MYB genes, called *VvMybA* followed by a number, that control berry coloration through *VvUFGT* transcriptional regulation [12, 13]. These previous studies showed that in colored berry cultivars, two paralogs (*VvMybA1* and *VvMybA2*) located at the BCL are functional. Given that *VvMybA1* and *VvMybA2* are two neighboring genes, they are largely inherited together and can be considered a block or haplotype. The haplotype C-N containing both functional *VvMybA1c* and *VvMybA2r* is able to activate *VvUFGT* expression and to produce berry skin pigmentation [14].

In white-skinned berry cultivars, the two functional genes, *VvMybA1* and *VvMybA2*, are mutated and constitute haplotype A (HapA). In the case of *VvMybA1* from HapA (*VvMybA1_HapA* or *VvMybA1a*), gene expression is repressed as a consequence of the insertion of the retrotransposon *Gret1* into the promoter region [15]. For *VvMybA2_HapA*, two nonsynonymous mutations inactivate the protein [12]. HapA is the major haplotype responsible for white-skinned berry cultivars, as it is homozygous in almost all white grape varieties [12]. However, there are a few exceptions. First, in the case of clonal variation, some white-skinned clones originate from black-skinned cultivars through mutations (e.g. 'Pinot noir' > 'Pinot blanc'). In these cases, the underlying molecular mechanism is fully understood and involves a large deletion at the BCL [16–18]. Second, Lijavetsky et al. described the allele *VvMybA1_SUB* in 'Sultanina' and reported four white-skinned

berry cultivars not homozygous for HapA [19]. The *VvMybA1_SUB* allele might belong to an independent putative haplotype, and was named haplotype F (HapF) [20]. Knowledge of HapF is limited, and several aspects remain unknown. For example, what about other *VvMybA* genes that might be present at the BCL for this haplotype?

In this study, we address these questions through a combination of PCR assays, Sanger sequencing, Oxford nanopore long-read sequencing (ONT), *de novo* assembly, whole genome sequencing (WGS), and transcriptomic approaches. We analyzed data from more than 500 cultivars originating from diverse countries around the world. We then reconstructed BCL for two cases: (i) HapF in a black-skinned cultivar that originated from the Alps and (ii) HapF from a white-skinned cultivar 'Khusaine Belyi'. We found that HapF in the white-skinned berry cultivar has undergone a large deletion that removed the majority of *VvMybA* genes at the BCL. In summary, HapF could be subdivided into three subhaplotypes—a non-functional HapF^{DEL} and two functional subhaplotypes, HapF1 and HapF2—with contrasting evolutionary histories. Finally, our results showed at least two origins for white grape cultivars in *V. vinifera*, contrary to expectations.

Results

The *VvMybA1_SUB* allele is present in colored-skinned and white-skinned berry cultivars

To estimate the geographical distribution and frequency of the *VvMybA1_SUB* allele, 528 *V. vinifera* accessions selected to represent the different origins from our grapevine collections were analyzed. Four different *VvMybA1* alleles were observed (Fig. 1). We identified 71 different accessions carrying the *VvMybA1_SUB* allele (Table S1). The *VvMybA1_SUB* allele frequency was 7%, lower compared to other alleles (e.g., 66% for the non-functional white allele *VvMybA1a* and 27% for the functional allele *VvMybA1c*). One cultivar was of particular interest: two alleles, *VvMybA1_SUB* and *VvMybA1a*, were detected in leaves of 'Humagne gris', whereas only the white allele *VvMybA1a* was detected in root extracts.

The *VvMybA1_SUB* allele was observed in cultivars originating from diverse countries. We did not find any French or German cultivars carrying *VvMybA1_SUB*. Only two Spanish cultivars ('Listan Prieto' and 'Mollar Cano') and one cultivar from Portugal ('Tinta Francisca') were shown to carry *VvMybA1_SUB*. By

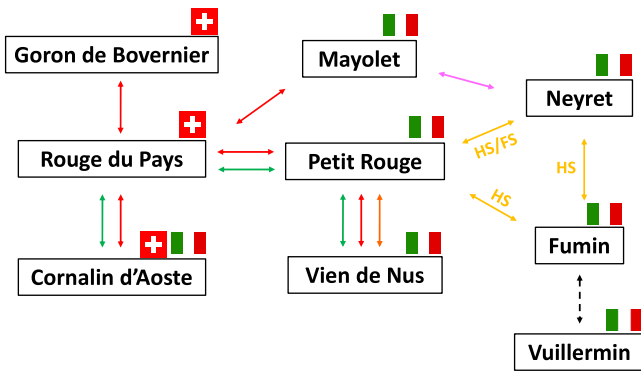


Figure 2. Genetic relationships between nine black-skinned cultivars from the Alps region according to the literature (if not specified, each arrow corresponds to a parent/offspring relationship according to different sources: Raimondi et al. [22] in yellow, Onofrio et al. [23] in green, Lacombe et al. [24] in red, Cipriani et al. [25] in violet and the dashed line indicates that at least one allele is shared across 9 SSR markers, as referenced on www.vivc.de). All nine cultivars carry the *VvMybA1_SUB* allele. HS and FS stand for half or full sibling. Flags indicate where each cultivar is grown: Switzerland (Valais) and/or Italy (Aosta Valley).

contrast, *VvMybA1_SUB* was identified in several cultivars from Italy (Table S1). Furthermore, this allele was identified in nine black-skinned cultivars from the Alps region (i.e. ‘Mayolet’, ‘Petit Rouge’, ‘Rouge du Pays’, ‘Goron de Bovernier’, ‘Cornalin d’Aoste’, ‘Neyret’, ‘Fumin’, ‘Vuillermin’, and ‘Vien de Nus’). Some of these genotypes are cultivated on both sides of the Swiss–Italian border (Valais and Aosta Valley). The nine alpine cultivars belong to a group of genetically closely related genotypes as illustrated by the IBD estimates (Fig. 2, Table S2). By comparing the proposed pedigrees of these cultivars with allelic composition data at *VvMybA1*, we identified a discrepancy. The cultivar ‘Rouge du Pays’ (syn. ‘Cornalin du Valais’) was found to have a *VvMybA1_SUB* / *VvMybA1c* genotype despite the suggested parents cv. ‘Mayolet’ and ‘Petit Rouge’ [21], both having a *VvMybA1_SUB* / *VvMybA1a* genotype. The plant material was genotyped with nine genome-wide SSR markers to verify the identity for trueness-to-type of cv. ‘Mayolet’, ‘Petit Rouge’, and ‘Rouge du Pays’ (<http://www.vivc.de/>). To further investigate the pedigree, nine additional SSR markers were analyzed, among which four markers were incompatible with the pedigree suggested by Vouillamoz et al. [21] for the cultivar ‘Rouge du Pays’ (Fig. S1).

Combining our analyses with published data (Table S3), we found that among 62 cultivars sharing genotype *VvMybA1_SUB* / *VvMybA1a*, 16 accessions had white-skinned berries, eight had light-colored-skinned berries (i.e. red or rose), and 38 had black-skinned berries. Comparative sequence analysis of the *VvMybA1_SUB* allele showed that the color difference could not be explained by variation in coding sequences of gene *VvMybA1*, given that they were identical. The co-occurrence of colored and white-fruited phenotypes among cultivars with genotype *VvMybA1_SUB* / *VvMybA1a* might indicate additional regulatory loci controlling berry skin color.

The berry color locus of haplotype F in alpine black-skinned berry cultivars

The BCL region was further analyzed in a homozygous genotype (*VvMybA1_SUB/VvMybA1_SUB*) derived from an alpine black-skinned cultivar. First, using PCR analysis, three *MybA*-related sequences, including the complete coding region, were obtained for the following genes: *VvMybA1* (PQ072838, 1820 bp), *VvMybA2* (PQ072839, 2361 bp), and *VvMybA3* (PQ072840, 2072 bp). Given

that *VvMybA1*, *VvMybA2*, and *VvMybA3* are adjacent genes, they are inherited together and can be considered haplotypes. The different haplotypes described for the BCL are summarized in Table 1, along with their allelic composition. The analysis of the coding sequences and protein products of the three genes from HapF are presented in Fig. 3. We found that (i) *VvMybA1_SUB* (= *VvMybA1_HapF*) encoded a protein of 250 amino acids in length; (ii) *VvMybA2_HapF* had a similar structure and length as *VvMybA2* from haplotype C-N: the duplication of a 282 bp-portion of the C-terminal domain in *VvMybA2_HapF* is of the same size as *VvMybA2r* from haplotype C-N [12]. Further, *VvMybA2_HapF* did not show the CA deletion and the mutation R- > L at position 44 of the protein described for the white allele *VvMybA2w* [12]; and (iii) contrary to what has been described for *VvMybA3* in other haplotypes (C-N, A), *VvMybA3_HapF* encoded a protein of similar length to *VvMybA1* due to the absence of the deletion of 209 bp observed in the third exon [12].

Second, the homozygous genotype was analyzed using ONT long-read genome sequencing. This sequencing experiment was conducted using a complete flow cell and generated 4.7 million reads (N50: 10.4 kb, passed bases: 22.5 Gb). After a long read de novo assembly, one contig (length: 3.8 Mbp) was identified to correspond to a part of chromosome 2 containing the color berry locus (Fig. S2). At this locus, nine different *VvMybA*-like sequences were identified over a region of approximately 138 kb. The sequences of those nine *VvMybA* genes were polished and corrected manually at the base-pair level using Illumina short read to correct long read sequencing errors. A comparison between the three sequences obtained by Sanger sequencing of PCR amplicons and genome assembly indicates a 100% identity over 6253 bp between the two approaches. Both berry color haplotypes (HapF vs. HapA in PN40024.v4) were compared using a dotplot (Fig. S3), and the inferred genomic organization from HapF is depicted in Fig. 4. The MYB sequence cluster organization for HapF is different from what has been reported for HapA. First, the order of the MYB sequences is not conserved between both haplotypes (Fig. 4, Fig. S3). Second, the number of MYB sequences in the cluster is not identical between haplotypes (8x for HapA or HapC-N, 9x for HapF). Third, at the BCL of HapF, we observed a tandem duplication (6.1 kb, 6.4 kb, 90% nucleotide identity) in the region containing *VvMybA4* (Fig. S3), resulting in two gene copies, denoted *VvMybA4a* and *VvMybA4b*. Finally, one MYB sequence from HapF, *VvMybA13*, has no close homolog in HapA (Fig. 4) and is distantly related to the *VvMybA1-2-3* and *VvMybA4-11* groups (nucleotide identity: 60–78%).

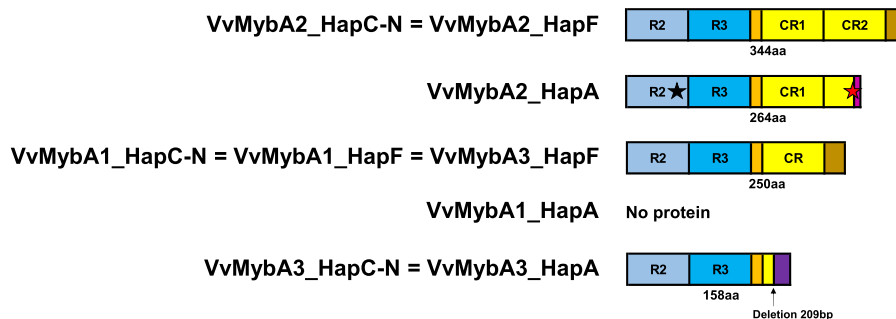
HapF was analyzed for transposable elements (TE). Four complete retrotransposons (with tandem site duplication and long terminal repeat (LTR) on both sides) were found in HapF that are not present in HapA (Fig. 4). The insertion times of the four intact LTR retrotransposons were estimated by comparing their LTR nucleotide divergences (Table S4). Insertion age estimates for these TE ranged from 0.19 to 1.19 million years ago. For comparison, using the same method, the insertion time of the retroelement *Gret1* described in HapA and partially responsible for the white-skinned berry phenotypes was estimated to be 0.15 million years ago.

Identification of a large deletion at the berry color locus of white-skinned cultivars bearing allele *VvMybA1_SUB*

To determine the portion of chromosome 2 around the *VvMybA1_SUB* gene in a white-skinned berry cultivar, cv. ‘Khusaine Belyi’

Table 1. Summary of the different haplotypes at the BCL. Allelic composition is given for every haplotype together with an example of a cultivar bearing it. *Gret1* is a retrotransposon

Haplotype	Species	Example of acultivar	VvMybA1	VvMybA2	VvMybA3	Berry skin color	Comments
HapA	<i>Vitis vinifera</i>	'Chasselas'	VvMybA1a: <i>Gret1</i> insertion in the promoter region, nonfunctional	2 nonsynonymous mutations, nonfunctional	209 bp deletion in the third exon, nonfunctional	Not able to trigger anthocyanin production	
HapB	<i>Vitis vinifera</i>	'Chardonnay rose'	VvMybA1b: <i>Gret1</i> is partially excised	2 nonsynonymous mutations, nonfunctional	209 bp deletion in the third exon, nonfunctional	Partially able to trigger anthocyanin production	
HapC-N	<i>Vitis vinifera</i>	'Pinot noir'	VvMybA1c: functional	VvMybA2r: functional	209 bp deletion in the third exon, nonfunctional	Trigger anthocyanin production	
HapD	<i>Vitis vinifera</i>	'Pinot blanc'	Absent, large deletion at the BCL	Absent, large deletion at the BCL	Absent, large deletion at the BCL	Not able to trigger anthocyanin production	
HapE1	<i>Vitis labrusca</i>	'Concord'	Absent, large deletion at the BCL	VlMybA1-2	VlMybA1-3	Trigger anthocyanin production	
HapF1	<i>Vitis vinifera</i>	'Saperavi'	VvMybA1_SUB, likely functional	Likely functional	No 209 bp deletion, likely functional	Trigger anthocyanin production	No tandem duplication of VvMybA4
HapF2	<i>Vitis vinifera</i>	'Montepulciano'	VvMybA1_SUB, likely functional	Likely functional	No 209 bp deletion, likely functional	Trigger anthocyanin production	Tandem duplication of VvMybA4
HapF ^{Del}	<i>Vitis vinifera</i>	'Sultanina'	VvMybA1_SUB, likely functional	Absent, large deletion at the BCL	Absent, large deletion at the BCL	Not able to trigger anthocyanin production	

**Figure 3.** Representation of the predicted MybA proteins produced from MYB genes at the color locus on chromosome 2, depending on the haplotype. Colored boxes are used to denote similar regions. R2 and R3 refer to repeats in c-Myb. The C-terminal domain (CR) is repeated in *VvMybA2_HapC-N* and *VvMybA2_HapF*. The black star in *VvMybA2_HapA* indicates a non-conservative change (R⁴⁴L), and the red star stands for a dinucleotide deletion introducing a premature stop codon. The protein length is given in amino acids (aa). Haplotype A produces no *VvMybA1* protein, given the insertion of a transposable element in the promoter region of the gene. *VvMybA3* in haplotypes C-N and A lacks most of the C-terminal domain, due to a 209 bp deletion in the coding region of the gene. *VvMybA2* and *VvMybA3* encode proteins with a similar structure in both haplotypes F1 and F2. *VvMybA1_HapF* is present in all three subhaplotypes (F1, F2, and F^{DEL}; see Table 1) and also exhibits a similar structure.

was selfed to obtain a homozygous genotype (*VvMybA1_SUB* / *VvMybA1_SUB*). We then used ONT long-read sequencing with an entire flow cell producing 5.9 M reads (N50: 10.6 kb, passed bases: 30.7 Gb) for the *de novo* assembly. One contig (length: 3.9 Mbp) corresponded to part of chromosome 2 (Fig. S4), including the BCL. A comparison of the BCL of HapF with the newly assembled BCL sequence revealed a large deletion of approximately 76 kb (Fig. S5). Therefore, this haplotype containing the partial deletion was named HapF^{DEL}. The genomic organization of the BCL for this haplotype is depicted in Fig. 5. Among the nine MYB sequences identified at the BCL previously for HapF, only three are present in HapF^{DEL}, namely *VvMybA1*, *VvMybA9*, and *VvMybA13*. The three sequences were highly similar to HapF (pairwise nucleotide iden-

tity: 98.6% to 99.3%; Fig. 5). The deleted segment mapped to 1.4 kb upstream of the gene *VvMybA3* and extended 10.8 kb downstream of the gene *VvMyb4b*. Thus, the region containing the 6 MYB sequences (*VvMybA3*, *VvMybA11*, *VvMybA10*, *VvMybA2*, *VvMybA4a*, and *VvMybA4b*) was absent from HapF^{DEL} compared to HapF.

To differentiate HapF from HapF^{DEL}, we developed a PCR assay that specifically targeted *VvMybA3* from HapF using specific INDELS (Fig. S6). The assay confirmed the absence of *VvMybA3_HapF* in genotypes HapA/HapA and HapC-N/HapA (data not shown). We used this assay across several accessions found to carry *VvMybA1_SUB* (Table S1). Among the 51 accessions with genotype *VvMybA1_SUB/VvMybA1_HapA*, 33 accessions produced

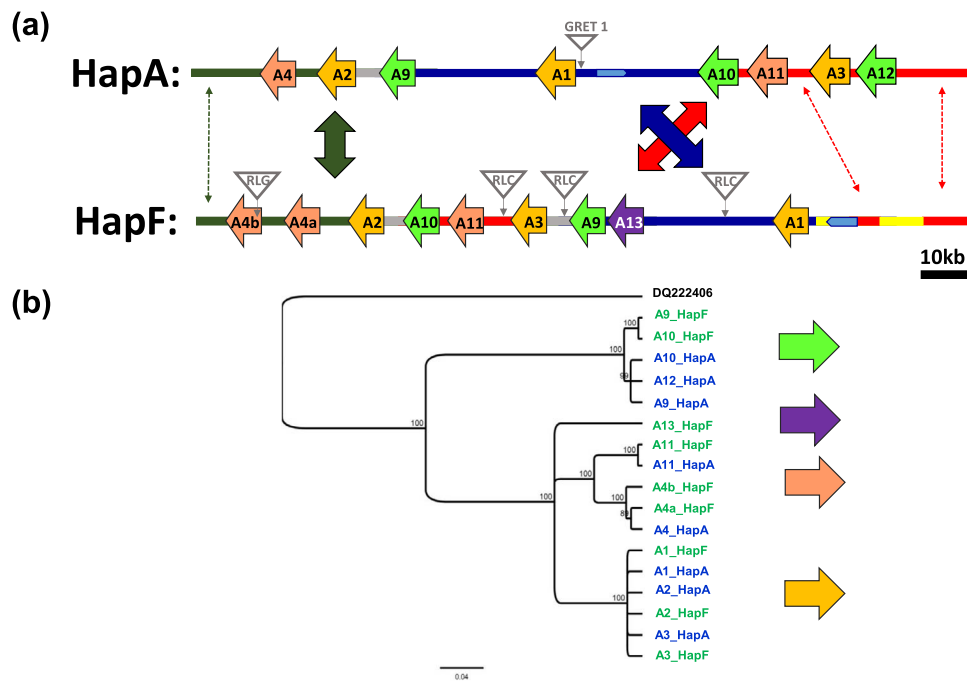


Figure 4. Organization of the berry color locus (BCL) on chromosome 2 for two haplotypes present in *Vitis vinifera*. HapA is the canonical non-functional haplotype from PN40024, while haplotype F is the one containing *VvMybA1.SUB*. **a** Schematic representation of the cluster of *MybA* genes (denoted here by A followed by a number) found in both haplotypes. Similar colors denote regions with similarities. The grapevine retrotransposon (Gret1) is shown in the *VvMybA1* promoter region of haplotype A. Transposable element insertions specific to haplotype F are shown as gray triangles, and two superfamilies were identified: Copia (RLC) and Gypsy (RLG); **b** Phylogenetic tree constructed from the different nucleotide sequences of *MybA* genes identified at BCL for both haplotypes A and F. The sequences are colored according to the haplotypes in which they have been identified (HapA in blue and HapF in green). *MybA75* (DQ222406) from *Arabidopsis thaliana* is used as the outgroup. The scale bar shows the number of substitutions per site.

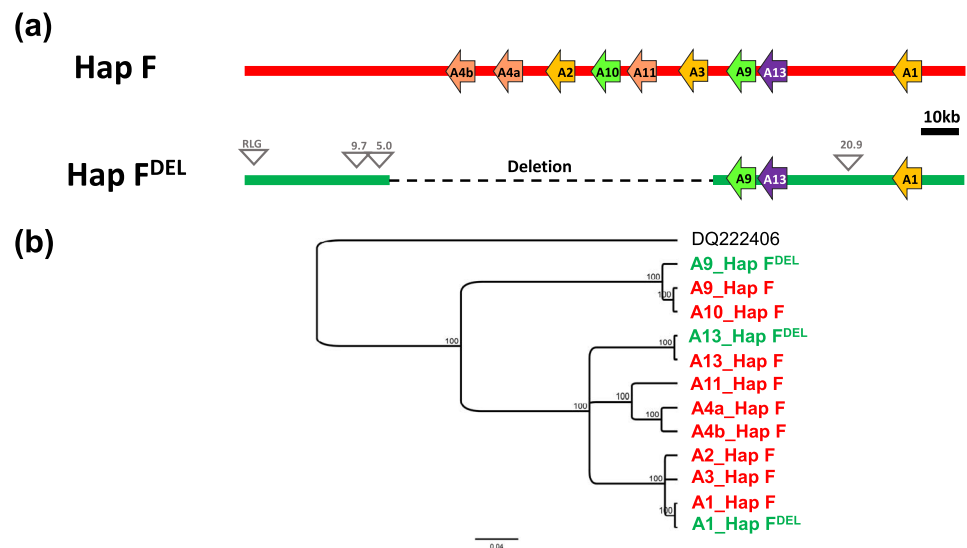


Figure 5. Organization of the berry color locus (BCL) for haplotype F compared to F^{DEL} . **a** Schematic representation of the cluster of *MybA* genes (denoted here by A followed by a number) found at the BCL. The deleted region in $HapF^{DEL}$ compared to HapF is indicated with a dashed line. Insertions specific to haplotype F^{DEL} are shown as gray triangles (RLG for Gypsy superfamily), for other insertions, size (in kb) is written above each insertion). **b** Phylogenetic tree constructed from the different nucleotide sequences of *MybA* genes identified at the BCL from both haplotypes F and F^{DEL} . The sequences are colored according to the haplotype in which they have been identified (haplotype F in red and haplotype F^{DEL} in green). *MybA75* (DQ222406) from *Arabidopsis thaliana* is used as the outgroup. The scale bar shows the number of substitutions per site.

positive outcomes in the assay, indicating the presence of the gene *VvMybA3_HapF*, and all these accessions presented a black-fruited phenotype. Among the 18 accessions lacking *VvMybA3_HapF*, we found 16 genotypes producing white-skinned berries and 5 light-colored (red or rose) berries. No black-skinned berries were produced from genotypes lacking *VvMybA3_HapF* (Table S1). Due to the very similar sequences between the different *VvMybA2*

alleles, we were unable to design a PCR assay to specifically distinguish the gene *VvMybA2_HapF*. Nevertheless, we examined the whole genomic sequencing data of seven accessions harboring $HapF^{DEL}$ from various geographical origins (Table S8). The $HapF^{DEL}$ appeared similar in the seven accessions, showing the same deletion pattern. $HapF^{DEL}$ was not found in western European cultivars used for wine making but was present in cultivars

Table 2. Gene expression data (TPM, transcripts per million) in berry skin at six weeks after veraison for four cultivars. BCL stands for berry color locus on chromosome 2

Cultivar	Genotype at BCL	Skin berry color	Gene/allele expression (TPM)						
			Haplotype F/F ^{DEL}			Haplotype A			
			VvMybA1	VvMybA2	VvMybA3	VvMybA1	VvMybA2	VvMybA3	UFGT
'Cornalin d'Aoste'	HapF/HapA	Black	33	98	104	n. d.	81	218	141
'Listan Prieto'	HapF/HapA	Black	2	23	95	n. d.	35	70	149
'Otcha Bala'	HapF ^{DEL} /HapA	White	9	n. d.	n. d.	n. d.	18	80	0.4
'Khusaine Belyi'	HapF ^{DEL} /HapA	White	5	n. d.	n. d.	n. d.	24	85	0.4

originating from Asia (mainly Caucasia and central Asia) used as table grapes (Table S1).

Allele VvMybA1_SUB is expressed at a low level in both white- and black-skinned cultivars

To study MybA gene expression in the skin after veraison, RNA-Seq transcriptome analysis was performed on four cultivars, two black-skinned (cv. 'Cornalin d'Aoste' and 'Listan Prieto') with genotype HapF/HapA at the BCL and two white-skinned cultivars (cv. 'Khusaine Belyi' and 'Otcha Bala') with genotype HapF^{DEL}/HapA. In those transcriptomes, based on RNA read alignments, no evidence was found for sequences VvMybA4a, VvMybA4b, VvMybA9, VvMybA10, VvMybA11, and VvMybA13 of HapF. Six different cDNAs (VvMybA1_HapF, VvMybA2_HapF, VvMybA3_HapF, VvMybA1_HapA, VvMybA2_HapA, and VvMybA3_HapA) were aligned. We identified private SNPs present in only one VvMybA allele (Table S5). We then estimated the proportion of each MybA-type sequence in the four transcriptomic datasets, averaging the allele frequencies of the corresponding private SNPs (Table S6). Using this information, we estimated the transcript per million metrics (TPM) for each gene/allele as a measure of gene expression (Table 2). As expected from the genomic analysis, neither VvMybA2_HapF nor VvMybA3_HapF transcription was detected in the white-skinned cultivars. By contrast, VvMybA1_HapF was detected in all four transcriptomic datasets, although at a lower rate compared to other expressed MybA genes. As anticipated, UFGT expression differed significantly between white- and black-fruited cultivars, emerging as one of the genes with the highest fold-change when comparing gene expression between the two groups (data not shown).

We also examined a transcriptomic dataset generated from cv. 'Sultanina' berry skin tissues after veraison [26]. No expression of VvMybA1_SUB was identified in this dataset (Table S6). To further analyze gene expression, we used two RT-PCR assays combined with Sanger sequencing. First, using primers specific to VvMybA1 (vvMybA1_f / vvMybA1_r), we specifically detected VvMybA1_HapF expression based on one SNP present in VvMybA1_HapF (Fig. S7). VvMybA1_HapF expression was observed in three white-skinned cultivars—'Khusaine Belyi', 'Otcha Bala', and 'LN33'—and two black-fruited cultivars—'Listan Prieto' and 'Cornalin d'Aoste'. However, the private SNP for VvMybA1_HapF expression was not detected in cv. 'Sultanina' (Fig. S7). Second, we developed another RT-PCR assay (vvMybA1_f / vvMybA1_Ex3_r) that produced a longer amplicon (530 bp) and specifically amplified only two cDNAs: VvMybA1_HapF and VvMybA3_HapF. Along the amplified region, 12 SNPs differentiated the two cDNAs. An inspection of the sequencing chromatograms at these 12 positions revealed double picks (Fig. S8). For both cv. 'Cornalin

d'Aoste' and 'Listan Prieto', each peak related to the private SNP of VvMybA1_HapF had a systematic lower intensity compared with the peak produced by allele VvMybA3_HapF.

Haplotype F is present in *V. vinifera* subsp. *sylvestris*

To investigate the evolution of MybA sequences, we examined the homologous region of BCL on chromosome 2 of four accessions of *V. sylvestris* [27] (www.grapegenomics.com). All four genotypes showed a VvMybA2 allele containing a duplicated portion (282 bp) of the C-terminal domain. Additionally, we identified two *V. sylvestris* accessions, DVIT3351.27 and O34-16, showing a very similar structure at the BCL as HapF described in this work (Fig. S9). In fact, eight MybA sequences were identified in those two *V. sylvestris* accessions that were highly similar (>99% nucleotide identity) to those from HapF described here. No evidence of segmental duplication was detected in the VvMybA4 region for both *V. sylvestris* accessions. Based on the different features observed for genes VvMybA4a and VvMybA4b, we propose an evolutionary scenario for this locus (Fig. S10). The first step was a tandem duplication, and using the same method for dating TE insertion, this tandem duplication was estimated to have occurred 1.2 million years ago. In the second phase, a TE inserted in the first exon of one copy of VvMybA4 and a 213-bp insertion occurred in the third exon of the other copy of VvMybA4. The age of this TE insertion was estimated at 0.69 million years ago by comparing the LTRs (Table S4) older than the *Gret1* insertion. We called HapF2 the haplotype that contained the tandem duplicated VvMybA4 and F1 the other haplotype.

To estimate the distribution, frequency, and type of haplotype F in *V. sylvestris*, we obtained archived sequence reads of WGS for 189 accessions (Table S7). In the WGS data for *V. sylvestris*, HapF2 was absent, and 40 accessions bearing HapF1 were detected (Table 3). HapF1 was absent in all tested accessions from Europe. By contrast, going east, in regions such as the Fertile Crescent (near the Mediterranean) and Caucasia, HapF1 was frequent in the *V. sylvestris* population. Furthermore, to estimate the distribution and type of HapF in *V. vinifera* subsp. *sativa*, we resequenced 5 alpine cultivars and analyzed 28 archived WGS for cultivars bearing VvMybA1_SUB (Table S8). Out of 33 cultivars, 7 had HapF^{DEL}; among the remaining 26 cultivars, HapF2 (containing the tandem duplication) was observed only in alpine cultivars and in cv. 'Montepulciano' (two independent WGS datasets). In all 17 other tested cultivars with diverse origins (i.e. from Spain to Uzbekistan), we found HapF1. Finally, we analyzed grape genome sequencing data related to archeological samples [28] and found that one cultivar, A33, carried HapF1 (Table S8).

Table 3. Haplotype F1 frequency detected in whole genomic sequencing (WGS) data in diverse accessions of *Vitis vinifera* subsp. *sylvestris* from different origin. The details of the studied WGS data are given in Table S7

Region/country where the accessions were collected	Number of WGS data examined	HapF1 detected (frequency in %)
Portugal	4	Not detected
Spain	20	Not detected
Tunisia	2	Not detected
France	10	Not detected
Europe	9	Not detected
Switzerland	5	Not detected
Germany	5	Not detected
Austria	4	Not detected
Italy	40	Not detected
Croatia	5	Not detected
Hungary	5	Not detected
Bulgaria	5	Not detected
Roumania	3	Not detected
Turkey	5	Not detected
Crimea	10	1 (10%)
Israel	11	7 (64%)
Iran	10	6 (60%)
Caucasia	6	3 (50%)
Armenia	10	8 (80%)
Azerbaijan	10	6 (60%)
Georgia	10	9 (90%)

Analysis of MybA genes at the berry color locus in *Muscadinia rotundifolia* and *Vitis labrusca*

We examined the homologous region of the BCL on chromosome 2 in *Muscadinia rotundifolia*. We used the data of chromosome-scale pseudomolecules published by Cochetel et al. [29] for the cultivar ‘Trayshed’. We compared haplotype H2 with chromosome 2 of PN40024. The two sequences were syntenic, except for a large inversion containing the BCL (Fig. S11). Haplotype 2 in *Muscadinia rotundifolia* cv. ‘Trayshed’ contains three MYB sequences similar to genes *VvMybA1* from *V. vinifera* (Fig. 6). Two of these sequences could represent functional genes and encode proteins of size 250 aa (MrMybA1) or 247 aa (MrMybA2) with high similarity to *VvMybA1* (identity with DQ886417: 92–97%). A third sequence (MrMybA3) represents a likely pseudogene, since a TE belonging to the *Copia* family has been inserted in the third exon. Regarding these three MybA1-like sequences, we observed that all had a second intron very similar to *VvMybA1_SUB* containing an insertion of 33 or 35 bp compared with the reference allele *VvMybA1c* (Fig. S12). Furthermore, the sequence *VvMybA13* from HapF in *V. vinifera* had a close homologous sequence in both haplotypes from *Muscadinia rotundifolia* cv. Trayshed (length: 1.2 kb; nucleotide identity: 92%) (Fig. 6). We made similar observations from the genomic data for another variety, *Muscadinia rotundifolia* cv. ‘Noble’ [30]: (i) the presence of three MybA1-like sequences, (ii) a second intron containing an insertion very similar to *VvMybA1_SUB*, and (iii) the presence of a homologous sequence of *VvMybA13_HapF*.

Finally, we examined the homologous region of the BCL on chromosome 2 of one individual of the species *V. labrusca*. We used the data published by Li and Gschwend (2023) for the genotype Grem-4. We compared the BCL region of Grem-4 with PN40024. Both regions had a high collinearity (Fig. S13). Seven MYB sequences were identified at the BCL of Grem-4 instead of eight for PN40024. This was explained by a large deletion (approximately 89 kb) that contained *VvMybA1* (Fig. S13). *VlMybA1-2* and *VlMybA1-3*, two MYB sequences reported previously in *V. labrusca* [20], were 100% identical to the BCL region in Grem-4. As shown

by the dotplot analysis (Fig. S13), we suggest that *VlMybA1-2* and *VvMybA2* are orthologs; the same applies for the pair *VlMybA1-3* and *VvMybA3*. Contrary to what has been described in *V. vinifera* for *VvMybA2*, gene *VlMybA1-2* did not show the 282-bp duplicated segment but a 9-bp deletion in the third exon compared to *VvMybA2*.

QTL analysis of wine anthocyanin content

‘Artaban’ and ‘Divico’ are two new grape varieties with resistance to fungal pathogens. Both are black-skinned berry cultivars heterozygous at the BCL. Indeed, out of 187 genotypes from a cross between those two cultivars, 36 progenies were white-skinned and 151 were black-skinned berry cultivars. These observations are consistent with a genetic model consisting of a single locus and black fruited being dominant over white fruited phenotype with a segregation ratio of 3:1 (chi-squared value = 3.29, $p = 0.07$). We made wines over three seasons and measured their anthocyanin content. The genotype effect determining wine anthocyanin content was evident, given the correlation between trait values across years and among genotypes (Fig. S14). QTL analysis for wine anthocyanin content showed a major QTL on chromosome 2 in the region of the BCL. Haplotype composition at this position had an important effect on wine anthocyanin content. The black-fruited progenies were divided into homozygous at the BCL with two copies of a functional haplotype, and heterozygous at BCL with a functional and a non-functional haplotype (i.e., HapA) (Fig. S15). The mean anthocyanin content was significantly higher (+71% on average over three years, $p = 3 \times 10^{-13}$) in wines made from genotypes having two functional haplotypes compared to the ones having only one.

Discussion

In this study, we conducted a deep analysis of the diversity in *VvMybA1* alleles present in grapevine germplasm collections. Similar to other studies [19, 31, 32], our results showed that

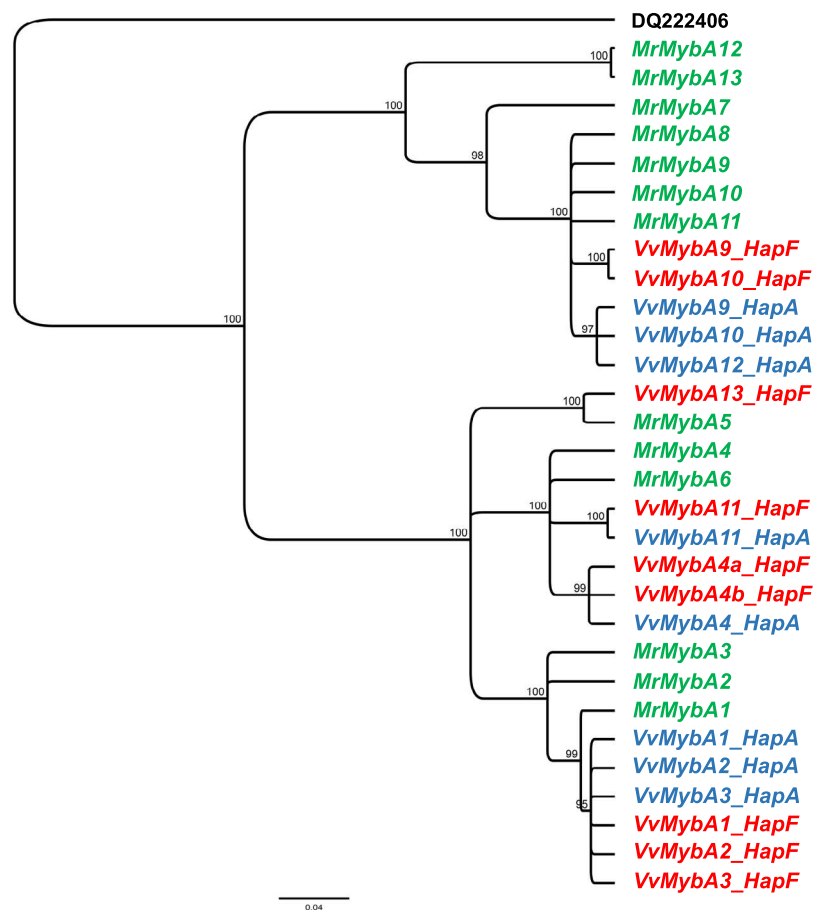


Figure 6. Phylogenetic tree constructed from different nucleotide sequences of *MybA* genes identified at BCL for *Vitis vinifera* and *Muscadinia rotundifolia* (H2) (Cochetel et al. [29]). The sequences are colored according to the haplotypes in which they have been identified. Haplotype A in blue and haplotype F in red were identified in *Vitis vinifera*, whereas haplotype H2 in green originated from *Muscadinia rotundifolia*. *MybA75* (DQ222406) from *Arabidopsis thaliana* is used as the outgroup. The scale bar shows the number of substitutions per site.

VvMybA1_SUB is a minor allele that is less frequently found than other alleles such as *VvMybA1a* and *VvMybA1c*. We observed this allele in various cultivars from Western Europe. For instance, ‘Listan Prieto’, an ancient Spanish cultivar, was found to carry allele *VvMybA1_SUB*. ‘Listan Prieto’ has also been cultivated for centuries in the Americas, where it is known by different synonyms, including ‘País’, ‘Criolla chica’, ‘Negra Corriente’, and ‘Mission’ [33, 34]. We also detected the *VvMybA1_SUB* allele in progenies of ‘Listan Prieto’ from South America (i.e. Criollas cultivars, e.g. ‘Quebranta’ and ‘Cereza’).

Valais in Switzerland and the Aosta Valley in Italy are neighboring regions in the Alps with a rich winegrowing heritage that dates back to at least the Roman era. During Roman times, a road was constructed over Mons Jovis, now known as the Great St Bernard Pass, which connected these two valleys. During the Middle Ages, pilgrims walked along *Via Francigena*, and this axis represented an important route between northern and southern Europe. On both sides of the border, indigenous grape cultivars have been cultivated there for centuries. Among these alpine cultivars, we identified nine black-skinned cultivars carrying HapF2 at the BCL. This haplotype-sharing pattern is the result of inheritance between close relatives. Indeed, these varieties were shown to belong to a group of genetically closely related cultivars [21–25]. This close genetic relationship between indigenous cultivars from both Valais and Aosta Valley was already proposed based on meticulous ampelographic observations at the beginning of

the 20th century [35]. Furthermore, Vouillamoz et al. [21] proposed that cv. ‘Rouge du Pays’ could be a progeny from a natural cross between cv. ‘Mayolet’ and cv. ‘Petit Rouge’. However, considering our results and a recent study using single nucleotide polymorphisms (SNP) [23], the pedigree of cv. ‘Rouge du Pays’ proposed by Vouillamoz et al. [21] should be revised. In some situations, recent works using SNP analysis do not support the parentage proposed using microsatellite data. One example is the different parentages proposed for ‘Sangiovese’ based on microsatellite markers [36, 37] that were invalidated by two recent studies using SNP analysis [23, 38]. Regarding cv. ‘Rouge du Pays’, we did not find any reliable parental pairs for this cultivar in our database. We conclude, therefore, that at least one of the parents of cv. ‘Rouge du Pays’ is unknown, probably representing an extinct cultivar.

Our results of RNA-Seq analysis showed that, among the nine *MybA*-like sequences from HapF2, only three similar genes were expressed in the skin after veraison: *VvMybA1*, *VvMybA2*, and *VvMybA3*. *VvMybA2_HapF* resembles the functional allele *VvMybA2r*, harboring neither the CA deletion nor the mutation R⁴⁴->L⁴⁴ [12, 39]. Both *VvMybA1_HapF* and *VvMybA3_HapF* encode a protein of 250 aa in length very similar to the functionally validated protein *VvMybA1* identified in other haplotypes [8, 12, 20]. We hypothesize that in the case of HapF, three adjacent *MybA* genes could be involved in activating anthocyanin production in berry skin. Functional assays should be performed in the future to verify this hypothesis. Contrary to what has been observed for

other haplotypes in *V. vinifera*, *VvMybA3* in HapF does not contain the 209-bp deletion in the third exon. Interestingly, previous studies and our findings have highlighted this characteristic in an ortholog of *VvMybA3* in haplotype E1 from *V. labrusca* [20, 40].

VvMybA1_SUB gene expression was detected in all studied cultivars (cv. 'Khusaine Belyi', 'Otcha Bala', 'Cornalin d'Aoste', 'Listan Prieto', and 'LN33') except for 'Sultanina'. Our results for 'Sultanina' confirmed the observations made from a previous work [19]. Compared to other expressed *MybA* genes, *VvMybA1_SUB* gene expression occurred at a lower rate in berry skin. A previous study also reported a low transcript level for *VvMybA1_SUB* in cv. 'Koshu' compared to the reference allele *VvMybA1c* in 'Cabernet Sauvignon' [41]. The coding part of *VvMybA1_SUB* is identical in HapF and HapF^{DEL}; on the protein level, *VvMybA1_SUB* showed 100% similarity (BLOSUM62 > 0) compared to *MYBA* genes that were functionally tested and shown to trigger anthocyanin production [12]. Furthermore, no obvious differences were detected in the promoter region of the gene *VvMyb1_SUB* between HapF and HapF^{DEL}. We propose, therefore, the following hypothesis to account for the *VvMybA1_SUB* gene expression and the white-skinned phenotype observed: *VvMybA1_SUB* is functionally active, but its transcript level is not sufficient to activate anthocyanin synthesis via UFGT gene induction. The activation of anthocyanin production by *MybA* transcripts is dose-dependent, based on our results that showed wine anthocyanin content was higher in homozygous genotypes at BCL with two functional haplotypes compared to those with only one (Fig. S15).

The anthocyanin biosynthesis pathway is well conserved in plants, and *MYB* transcription factors have been found to play critical roles in anthocyanin accumulation in different horticultural plants. Various allelic variants of the key regulatory *MYB* transcription factors with their respective phenotypes were identified for different crops [42, 43]. For instance, Liu et al. attributed the yellow-skinned fruit (absence of anthocyanin) phenotype of sweet cherry (*Prunus avium*) to a nonfunctional allele due to a large deletion encompassing the *MYB* regulatory gene [44]. For grapevine, HapF^{DEL} described in this work, represents a loss-of-function haplotype responsible for the lack of anthocyanin accumulation in berry skin. BCL showed a high genomic plasticity, and structural variants are common at this locus, as suggested by our results for HapF^{DEL} and the haplotype from *V. labrusca* Grem-4. In grapevines, some nonfunctional or partially functional haplotypes involving large deletions encompassing the BCL have already been reported to be involved in somaclonal variations [45–47]. Interestingly, in our study, we encountered a similar case with cv. 'Humagne gris', a bronze-colored somatic mutant of the cv. 'Cornalin d'Aoste' [48], which had a chimeric structure [49]. For 'Humagne gris', the L1 cell layer had HapF2 at BCL, whereas a deletion occurred in L2 cells eliminating the *MybA* genes of this haplotype. Ancient writings mentioned 'Oriou gris', a pale-colored variety, being cultivated in Aosta Valley during the XIX century [50]. 'Oriou gris' was most probably a somatic mutant of 'Petit Rouge', which was likely derived from it via a mechanism similar to what has been described here for 'Humagne gris'.

Unlike HapA, the main white berry-skinned haplotype containing *Gret1*, which is present in both table and wine grape cultivars, HapF^{DEL} is found only in table grape varieties and did not migrate to western Europe. Therefore, HapF^{DEL} likely appeared quite recently in the history of grape domestication, probably after the table and wine grape cultivars diverged; this divergence point was estimated to be around 2600 years ago [51]. The most likely evolutive scenario for HapF^{DEL} is that it appeared somewhere in

Asia, where it was then selected by humans and disseminated along the ancient Silk Road trade route in the direction of East Asia. Domesticated *V. vinifera* probably reached China and Japan during the last two millennia. To date, the earliest evidence of the presence of *V. vinifera* in China dates back to the second century BCE in the Turpan District in Xinjiang Province [52]. The cv. 'Khusaine Belyi' was introduced in China at least as early as 900 CE [53]. Further evidence shows that a cultivated *V. vinifera* accession having HapF^{DEL} naturally hybridized with a descendant of the Chinese wild species *Vitis davidii* to give birth to 'Koshu' cultivated at least since the 12th century in Japan [54].

Grapevine domestication and viticulture spreading result from a complex process, and some aspects are still highly debated. For instance, some works suggested a single domestication event in the Near East [55–57], whereas Dong et al. [53] proposed two centers of domestication for grapevine, the first one in the Transcaucasus, and the second in the Fertile Crescent (near the Mediterranean). Based on genetic and archeological evidence, researchers generally accept that the Near East region is the primary domestication center(s), after which domesticated grapevine spread to other regions following the main civilizations along human migration routes. Domesticated grapevines spread to Europe around 3000 years ago during the Late Bronze Age [58]. In this study, we found that HapF1 at the BCL had a high frequency (>50%) in the *V. sylvestris* population sampled in the Transcaucasus region and Israel. Furthermore, our results showed that HapF1 was present in an archeological cultivar found in the Middle East dating back to late antiquity (8th century CE). Thus, we can reasonably hypothesize that HapF1 from *vinifera* varieties originated from *sylvestris* populations domesticated in the Near East. It was then disseminated throughout the world as winegrowing spread. We found current *vinifera* varieties bearing F1 from Spain to Uzbekistan (Fig. S16). Our results confirmed the east-to-west gene flow following the spread of domesticated forms of *V. vinifera*.

HapF2, however, followed a different pattern of distribution. It was not detected in the *sylvestris* population but was observed in cultivated varieties but only in a restricted geographical area (in central and north of Italy (Aosta region) and in Switzerland (Valais) at the border with Italy). HapF2 was found in nine closely related alpine cultivars. In addition, only cv. 'Montepulciano', which is not directly related to the alpine cultivars, showed the presence of HapF2. This cultivar is one of the most important varieties in central Italy and is the second black-skinned variety planted in terms of surface area in Italy after 'Sangiovese'. To account for these observations, we can hypothesize that F2 would have originated from a *sylvestris* population in the Italian peninsula; this population is either extinct or has not been captured in the samples we analyzed. Given that cultivated grapes moved into Europe (the origin of Italian viticulture is thought to date back to the Etruscans, around 8th century BCE), it is plausible that western European *vinifera* cultivars encountered local *sylvestris* populations and hybridized with them along migration routes. This putative hybridization could have transferred HapF2 into the cultivated compartment. This putative scenario would be in accordance with a growing body of literature [51, 53, 57, 59, 60] showing that western European *vinifera* cultivars experienced introgression from local *sylvestris*. Our scenario for HapF2 is in agreement with previous observations made by Magris et al. [56] that the highest proportion of western *sylvestris* ancestry was found in autochthonous varieties from central and northern Italy.

Overall, our findings offer valuable insights into the genetic mechanisms underlying berry skin coloration in *Vitis vinifera*,

enhancing our understanding of grapevine domestication history. We identified a nonfunctional haplotype (HapF^{DEL}) responsible for the white-skinned berry phenotype, described here for the first time. By analyzing the geographic distribution of BCL haplotypes, we propose that white-skinned grape cultivars originated independently at least twice during domestication. Furthermore, an improved understanding of the genetic model controlling berry skin color holds significant potential for advancing breeding programs aimed at producing high-quality fruits.

Materials and methods

Plant materials

The study was mostly performed using materials originating from two national grapevine repositories: at Agroscope in Pully (VD) in Switzerland and at INRAE in Domaine de Vassal near Montpellier in France. Furthermore, a few accessions were provided from the germplasm repository at JKI Geilweilerhof (Siebeldingen, Germany) and from the Institut Agricole Régional (Aosta, Italy). The genotypes 576P (['Rouge du Pays' × 'Bronner'] × 'Voltis') and 'Khusaine Belyi' were selfed to produce homozygous seedlings at the BCL.

To study the genetic component of anthocyanin content in wine, 187 progenies from the cross between cv. 'Artaban' and 'Divico' were planted (5 stocks per genotype) in 2017 in the field at Pully in Switzerland (46° 30' 49" N, 6° 39' 59" E). Microvinifications were carried out using a standardized protocol during three vintages, 2020, 2021, and 2022, and wines were analyzed for anthocyanin content using the spectrophotometric method described by Puissant and Leon [61].

DNA preparation, PCR analysis, and sequencing of *VvMybA1*, *VvMybA2*, and *VvMybA3* alleles

Genomic DNA was isolated from the leaves of field-grown plants or the roots of potted plants in the case of cv. 'Humagne gris' using a rapid CTAB procedure [62]. Specific primers were used for the amplification of the different *VvMybA* genes (Table S9). PCR was performed according to the authors' instructions (Table S9). Amplified DNA was separated on 1.5% agarose gels, stained with ethidium bromide, and directly Sanger sequenced by Fasteris SA (Geneva, Switzerland).

MinION and Illumina DNA sequencing

DNA was extracted from young leaves using a CTAB procedure [63]. The extract was treated with 1 mg/mL RNase A for 30 min at 37°C. Illumina sequencing of the homozygous genotype (*VvMybA1_SUB* / *VvMybA1_SUB*) derived from selfing of the breeding line 576P was performed by Novogene (England) using TruSeq DNA library preparation, followed by a NextSeq 6000 sequencing run (2 × 150 bp). This WGS dataset consisted of 71.5 million bp. For long read sequencing, we used the technology of Oxford Nanopore Technologies (ONT), as described by Debonneville et al. [63]. Long reads from ONT were *de novo* assembled using Flye v2.8.3 [64] with default parameters. To correct possible assembly/ONT sequencings errors at the BCL, Illumina sequences were mapped using Geneious Prime 2023.2.1 (Biomatters Ltd) and visually inspected.

Bioinformatic analysis

To identify MYB sequences at the BCL, we mapped the conserved part of *VvMybA1* (R2R3 parts of the gene corresponding to exon 1, intron 1, and exon 2) on the investigated contig using Geneious [65] with the highest sensitivity settings. TE annotation at BCL

was performed using EDTA [66]. The age of each LTR retrotransposon element was estimated based on the sequence divergence between their LTR pair [67]. Dotplots were used to compare two sets of sequences. We used either D-Genies [68] to compare entire chromosomes/contigs or Gepard v2.0 [69] to compare berry color locus regions. The nucleotide and protein sequences were aligned using MUSCLE V5.1 implemented in Geneious Prime 2023.2.1. Phylogenetics trees were computed using the UPGMA algorithm, Tamura-Nei genetic distance, and bootstrapping with 1000 replicates, as implemented in Geneious Prime 2023.2.1. The consensus tree was rooted with *AtMyb75* as the outgroup. Branches with less than 90% support value were collapsed.

In the analysis of the WGS data, every dataset was mapped using the Geneious mapper against *VvMybA* genes from HapF. To identify HapF, the alignment was visually inspected for the insertion of 33 bp in the second intron of *VvMybA1*; the other *VvMybA* alignments were then examined for confirmation of the presence of HapF. To differentiate the different F subhaplotypes, each alignment was inspected visually, and different criteria were considered: (i) reads spanning the junction of the two tandem copies for detecting the tandem duplication in the region *VvMybA4*; (ii) a SNP located at position 99 of the second intron for *VvMybA1_SUB*; (iii) reads spanning the small insertion of 213 bp in gene *VvMybA4a*, and (iv) reads spanning the junction between RLG transposon and the gene *VvMybA4b*. Identity-by-descent (IBD) analyses were performed on SNP calls retrieved from grapevine whole-genome sequencing data described previously. We followed GATK [70] best practices to call SNPs and subset these to a single SNP per 10 kb window along chromosomes retaining only SNPs with >90% genotyping rate. The filtered VCF file was used in PLINK 2.0 to calculate IBD values with the `—make-king` option [71].

Microsatellite analysis

We analyzed five nuclear simple sequence repeats (SSR) markers (VVih54, VVIq52, VViv37, VViv67, and VVMD28) to assess the parentage analysis of cv. 'Rouge du Pays'. DNA was extracted with the DNeasy Plant Kit (Qiagen) from the young expanded leaves. Amplification was performed on a TProfessional TRIO Thermocycler® (Biometra) and visualized using a 4300 DNA Analyser platform (LI-COR). Allele sizes were determined by comparison with known genotypes of standard cultivars.

VvMybA gene expression analysis in berry skin

Berry samples were taken from field-grown vines. Nine ripe berries of three sun-exposed bunches were collected 6 weeks after veraison. Berry skin was immediately separated from flesh and seeds and directly grounded in liquid nitrogen. Total RNA was extracted from 100 mg tissue using the RNeasy Plant Mini Kit (Qiagen). RT-PCR was performed following the manufacturer's instructions in one step, starting with 1 µg of total RNA. Each reaction contained the specific primers (Table S9), AMV RT (Promega), RNasin® Ribonuclease Inhibitor (Promega), and GoTaq® Green Master Mix (Promega). The amplified DNAs were separated on 1.5% agarose gel, manually selected according to their sizes, and Sanger sequenced by Fasteris SA (Geneva, Switzerland). For the RNA-Seq experiment, library preparation and transcriptome sequencing were performed at Fasteris (Geneva, Switzerland). Briefly, the stranded mRNA protocol (Poly A selection) was used according to the manufacturer's instructions for constructing cDNA libraries followed by pair-end sequencing (2 × 150 bp) on an Illumina Novaseq sequencer. Processed reads were mapped against the public transcriptome of *V. vinifera* PN4002412X.v2

[72] using Salmon v1.6.0. [73]. To evaluate the expression of individual alleles of *VvMybA1*, *VvMybA2*, and *VvMybA3*, we initially aligned the nucleotide sequences of all six alleles using MEGA X to identify private SNP (present only in one allele) and then generated a 'consensus' *VvMybA* expressed sequence (Table S5).

QTL analysis of wine anthocyanin content

Genomic DNA extraction from young, expanding leaves was performed using the Qiagen DNeasy 96 Plant Kit, according to the manufacturer's instructions (Qiagen S.A., Courtaboeuf, France). The 187-progeny population was genotyped using the genotyping-by-sequencing (GBS) method [74]. SNP calling was carried out with GATK [70] after read mapping to the PN40024.v4 reference genome. A genetic map was constructed with Lep-MAP3 [75] and QTL mapping was performed with the R package R/qtl [76]. Sample genotypes were analyzed at the QTL peaks based on the final VCF file used to build the map. The two classes of homozygotes versus heterozygotes at the BCL were sorted based on information from a biallelic SNP at the QTL peak.

Acknowledgements

The authors thank Cécile Marchal, director of INRAE grapevine collection of Vassal-Montpellier for the plant material and documentation, Dr Olivier Schumpp, head of the virology group at Agroscope for providing support and facilities, Dr Agnes Dienesné Nagy for analyzing wine anthocyanin content and Dr Franco Röckel for sharing plant material from the Geilweilerhof (Germany) germplasm and Zecca Odoardo from the Institut Agricole in Aosta (Italy) for exchanging plant material.

Author contributions

J.S.R. designed the experiment, managed the project, and wrote the manuscript. J.L.S., V.Z., T.L. and D.C. provided support, facilities, and financial resources. J.B. conducted the laboratory work for genomic sequencing and PCR analysis. T.L. and J.S.R. collected biological samples. D.R., J.B., and J.S.R. performed the ONT sequencing and transcriptomic analysis. D.R. and J.S.R. performed the data analysis. T.V. conducted the microvinifications. K.A. was responsible for genetic mapping and QTL analysis. E.D. performed the microsatellite analysis. D.C. conducted the WGS experiment and provided guidance on genome evolution. All authors reviewed, revised, and approved the final manuscript.

Data availability

DNA sequencing and RNA-Seq datasets were deposited in the Sequence Read Archive under Bioproject PRJNA1166439.

Conflict of interest statement

The authors declare no conflicts of interest.

Supplementary Data

Supplementary data is available at *Horticulture Research* online.

References

- Vogt T. Phenylpropanoid biosynthesis. *Mol Plant*. 2010;**3**:2–20
- Albert NW, Lafferty DJ, Moss SMA. et al. Flavonoids—flowers, fruit, forage and the future. *J R Soc N Z*. 2023;**53**:304–31
- Slinkard K, Singleton V. Phenol content of grape skins and the loss of ability to make anthocyanins by mutation. *Vitis*. 1984;**23**:173–5
- Guasch-Jané MR, Andrés-Lacueva C, Jáuregui O. et al. First evidence of white wine in ancient Egypt from Tutankhamun's tomb. *J Archaeol Sci*. 2006;**33**:1075–80
- Levadoux L. *La sélection et l'hybridation Chez la Vigne*. Montpellier: Imprimerie Charles Déhan; 1951:
- Sparvoli F, Martin C, Scienza A. et al. Cloning and molecular analysis of structural genes involved in flavonoid and stilbene biosynthesis in grape (*Vitis vinifera* L.). *Plant Mol Biol*. 1994;**24**:743–55
- Boss PK, Davies C, Robinson SP. Anthocyanin composition and anthocyanin pathway gene expression in grapevine sports differing in berry skin colour. *Aust J Grape Wine Res*. 1996;**2**:163–70
- Kobayashi S, Ishimaru M, Hiraoka K. et al. Myb-related genes of the Kyoho grape (*Vitis labruscana*) regulate anthocyanin biosynthesis. *Planta*. 2002;**215**:924–33
- Klemppnauer K-H, Gonda TJ, Michael Bishop J. Nucleotide sequence of the retroviral leukemia gene v-myb and its cellular progenitor c-myb: the architecture of a transduced oncogene. *Cell*. 1982;**31**:453–63
- Paz-Ares J, Ghosal D, Wienand U. et al. The regulatory c1 locus of *Zea mays* encodes a protein with homology to myb proto-oncogene products and with structural similarities to transcriptional activators. *EMBO J*. 1987;**6**:3553–8
- Doligez A, Bouquet A, Danglot Y. et al. Genetic mapping of grapevine (*Vitis vinifera* L.) applied to the detection of QTLs for seedlessness and berry weight. *Theor Appl Genet*. 2002;**105**:780–95
- Walker AR, Lee E, Bogs J. et al. White grapes arose through the mutation of two similar and adjacent regulatory genes. *Plant J*. 2007;**49**:772–85
- Fournier-Level A, Lacombe T, le Cunff L. et al. Evolution of the *VvMybA* gene family, the major determinant of berry colour in cultivated grapevine (*Vitis vinifera* L.). *Heredity*. 2010;**104**:351–62
- Azuma A. Genetic and environmental impacts on the biosynthesis of anthocyanins in grapes. *The Horticulture Journal*. 2018;**87**:1–17
- Kobayashi S, Goto-Yamamoto N, Hirochika H. Retrotransposon-induced mutations in grape skin color. *Science*. 2004;**304**:982
- Vezzulli S, Leonardelli L, Malossini U. et al. Pinot blanc and Pinot gris arose as independent somatic mutations of Pinot noir. *J Exp Bot*. 2012;**63**:6359–69
- Walker AR, Lee E, Robinson SP. Two new grape cultivars, bud sports of Cabernet Sauvignon bearing pale-coloured berries, are the result of deletion of two regulatory genes of the berry colour locus. *Plant Mol Biol*. 2006;**62**:623–35
- Carbonell-Bejerano P, Royo C, Torres-Pérez R. et al. Catastrophic unbalanced genome rearrangements cause somatic loss of berry color in grapevine. *Plant Physiol*. 2017;**175**:786–801
- Lijavetzky D, Ruiz-García L, Cabezas JA. et al. Molecular genetics of berry colour variation in table grape. *Mol Gen Genomics*. 2006;**276**:427–35
- Azuma A, Kobayashi S, Mitani N. et al. Genomic and genetic analysis of Myb-related genes that regulate anthocyanin biosynthesis in grape berry skin. *Theor Appl Genet*. 2008;**117**:1009–19
- Vouillamoz J, Maigre D, Meredith CP. Microsatellite analysis of ancient alpine grape cultivars: pedigree reconstruction of *Vitis vinifera* L. 'Cornalin du Valais'. *Theor Appl Genet*. 2003;**107**:448–54

22. Raimondi S, Tumino G, Ruffa P. et al. DNA-based genealogy reconstruction of Nebbiolo, Barbera and other ancient grapevine cultivars from northwestern Italy. *Sci Rep.* 2020;**10**:15782
23. D'Onofrio C, Tumino G, Gardiman M. et al. Parentage atlas of Italian grapevine varieties as inferred from SNP genotyping. *Front. Plant Sci.* 2021;**11**:11
24. Lacombe T, Boursiquot JM, Laucou V. et al. Large-scale parentage analysis in an extended set of grapevine cultivars (*Vitis vinifera* L.). *Theor Appl Genet.* 2013;**126**:401–14
25. Cipriani G, Spadotto A, Jurman I. et al. The SSR-based molecular profile of 1005 grapevine (*Vitis vinifera* L.) accessions uncovers new synonymy and parentages, and reveals a large admixture amongst varieties of different geographic origin. *Theor Appl Genet.* 2010;**121**:1569–85
26. Balic I, Vizoso P, Nilo-Poyanco R. et al. Transcriptome analysis during ripening of table grape berry cv. Thompson seedless. *PLoS One.* 2018;**13**:e0190087
27. Massonnet M, Cochetel N, Minio A. et al. The genetic basis of sex determination in grapes. *Nat Commun.* 2020;**11**:2902
28. Cohen P, Bacilieri R, Ramos-Madriral J. et al. Ancient DNA from a lost Negev Highlands desert grape reveals a late antiquity wine lineage. *Proc Natl Acad Sci.* 2023;**120**:e2213563120
29. Cochetel N, Minio A, Massonnet M. et al. Diploid chromosome-scale assembly of the *Muscadinia rotundifolia* genome supports chromosome fusion and disease resistance gene expansion during *Vitis* and *Muscadinia* divergence. *G3 (Bethesda).* 2021;**11**
30. Park M, Darwish AG, Elhag RI. et al. A multi-locus genome-wide association study reveals the genetics underlying muscadine antioxidant in berry skin. *Front Plant Sci.* 2022;**13**:969301
31. Lacombe, T., *Contribution à l'étude de l'histoire évolutive de la vigne cultivée (Vitis vinifera L.) par l'analyse de la diversité génétique neutre et de gènes d'intérêt.* 2012, Centre International d'Etudes Supérieures en Sciences Agronomiques: Montpellier p. 328.
32. Margaryan K, De Lorenzis G, Aroutiounian R. et al. Genetic analysis of the VvMybA1 gene in Armenian grapevines (*V. vinifera* L.). *Vitis.* 2015;**54**:49–50
33. Alejandra Milla T, Cabezas JA, Cabello F. et al. Determining the Spanish origin of representative ancient American grapevine varieties. *Am J Enol Vitic.* 2007;**58**:242–51
34. Lalla Hasna Z, Haddioui A, Rodríguez V. et al. Identification by SNP analysis of a major role for Cayetana Blanca in the genetic network of Iberian Peninsula grapevine varieties. *Am J Enol Vitic.* 2012;**63**:121–6
35. Berget A. Etude ampélographique des vignobles du Léman, du Valais et du val d'Aoste. *Revue du viticulture.* 1903;502
36. Vouillamoz J, Monaco A, Costantini L. et al. The parentage of 'Sangiovese', the most important Italian wine grape. *Vitis.* 2007;**46**:19–22
37. Bergamini C, Caputo AR, Gasparro M. et al. Evidences for an alternative genealogy of 'Sangiovese'. *Mol Biotechnol.* 2013;**53**:278–88
38. Crespan M, Mercati F, De Lorenzis. et al. Two main distinct evolutionary stories describe the Italian grapevine assortment. *Vitis.* 2023;**62**:30–6
39. Jiu S, Guan L, Leng X. et al. The role of VvMYBA2r and VvMYBA2w alleles of the MYBA2 locus in the regulation of anthocyanin biosynthesis for molecular breeding of grape (*Vitis* spp.) skin coloration. *Plant Biotechnol J.* 2021;**19**:1216–39
40. Azuma A, Udo Y, Sato A. et al. Haplotype composition at the color locus is a major genetic determinant of skin color variation in *Vitis × labruscana* grapes. *Theor Appl Genet.* 2011;**122**:1427–38
41. Shimazaki M, Fujita K, Kobayashi H. et al. Pink-colored grape berry is the result of short insertion in intron of color regulatory gene. *PLoS One.* 2011;**6**:e21308
42. Butelli E, Garcia-Lor A, Licciardello C. et al. Changes in anthocyanin production during domestication of citrus. *Plant Physiol.* 2017;**173**:2225–42
43. Castillejo C, Waurich V, Wagner H. et al. Allelic variation of MYB10 is the major force controlling natural variation in skin and flesh color in strawberry (*Fragaria* spp.) fruit. *Plant Cell.* 2020;**32**:3723–49
44. Liu C, Qi X, Song L. et al. Large-fragment deletion encompasses the R2R3 MYB transcription factor, PavMYB10.1, causes yellow fruits in sweet cherry (*Prunus avium* L.). *Sci Hortic.* 2023;**309**:111648
45. Zhou Y, Minio A, Massonnet M. et al. The population genetics of structural variants in grapevine domestication. *Nature Plants.* 2019;**5**:965–79
46. Röckel F, Moock C, Schwander F. et al. A 69 kbp deletion at the berry color locus is responsible for berry color recovery in *Vitis vinifera* L. cultivar 'Riesling Rot'. *Int J Mol Sci.* 2022;**23**:23
47. Röckel F. *Färberreben (Teinturiers) Sowie Rote Farbmutanten weißer Qualitätsrebsorten Entstanden Durch VvmybA-Bedingte Mutationen am Beerenfarbokus.* Julius Kühn-Institut: Quedlinburg (Deutschland); 2017:128
48. Maigre D. Humagne gris: première observation d'une forme grise de l'Humagne rouge en Valais. *Revue suisse de viticulture, arboriculture, horticulture.* 2005;**37**:153–5
49. Pelsy F. Molecular and cellular mechanisms of diversity within grapevine varieties. *Heredity.* 2010;**104**:331–40
50. Gatta LF. *Saggio Sulle Viti e Sui Vini Della Valle d'Aosta.* R. Società Agraria; Torino, 1838:
51. Zhou Y, Massonnet M, Sanjak JS. et al. Evolutionary genomics of grape (*Vitis vinifera* ssp. *vinifera*) domestication. *Proc Natl Acad Sci.* 2017;**114**:11715–20
52. Jiang H-E, Zhang YB, Li X. et al. Evidence for early viticulture in China: proof of a grapevine (*Vitis vinifera* L., Vitaceae) in the Yanghai Tombs, Xinjiang. *J Archaeol Sci.* 2009;**36**:1458–65
53. Dong Y, Duan S, Xia Q. et al. Dual domestications and origin of traits in grapevine evolution. *Science.* 2023;**379**:892–901
54. Goto-Yamamoto N, Sawler J, Myles S. Genetic analysis of East Asian grape cultivars suggests hybridization with wild *Vitis*. *PLoS One.* 2015;**10**:e0140841
55. Myles S, Boyko AR, Owens CL. et al. Genetic structure and domestication history of the grape. *Proc Natl Acad Sci.* 2011;**108**:3530–5
56. Magris G, Jurman I, Fornasiero A. et al. The genomes of 204 *Vitis vinifera* accessions reveal the origin of European wine grapes. *Nat Commun.* 2021;**12**:7240
57. Xiao H, Liu Z, Wang N. et al. Adaptive and maladaptive introgression in grapevine domestication. *Proc Natl Acad Sci USA.* 2023;**120**:e2222041120
58. Bouby L, Chabal L, Bonhomme V. et al. The Holocene history of grapevine (*Vitis vinifera*) and viticulture in France retraced from a large-scale archaeobotanical dataset. *Palaeogeogr Palaeoclimatol Palaeoecol.* 2023;**625**:111655
59. D'Onofrio C. *Introgression among cultivated and wild grapevine in Tuscany.* *Frontiers. Plant Sci.* 2020;**11**:11
60. Freitas S, Gazda MA, Rebelo MÃ. et al. Pervasive hybridization with local wild relatives in Western European grapevine varieties. *Sci Adv.* 7:eabi8584
61. Vivas N, Vivas N, Nonier M-F. Estimation and quantification of wine phenolic compounds. *Bull Org Int Vigne Vin.* 2003;**76**:281–303

62. Gambino G, Perrone I, Gribaudo I. A rapid and effective method for RNA extraction from different tissues of grapevine and other woody plants. *Phytochem Anal.* 2008;**19**:520–5
63. Debonneville C, Mandelli L, Brodard J. et al. The complete genome of the “Flavescence Dorée” Phytoplasma reveals characteristics of low genome plasticity. *Biology (Basel)*. 2022;**11**:
64. Kolmogorov M, Yuan J, Lin Y. et al. Assembly of long, error-prone reads using repeat graphs. *Nat Biotechnol.* 2019;**37**:540–6
65. Kearsse M, Moir R, Wilson A. et al. Geneious basic: an integrated and extendable desktop software platform for the organization and analysis of sequence data. *Bioinformatics.* 2012;**28**:1647–9
66. Su, W., Ou S., Hufford M.B., Peterson T., A tutorial of EDTA: extensive De novo TE annotator. *Methods Mol Biol*, 2021. **2250**: p. 55-67, New York, NY, Springer US.
67. SanMiguel P, Gaut BS, Tikhonov A. et al. The paleontology of intergene retrotransposons of maize. *Nat Genet.* 1998;**20**:43–5
68. Cabanettes F, Klopp C. D-GENIES: dot plot large genomes in an interactive, efficient and simple way. *PeerJ.* 2018;**6**:e4958
69. Krumsiek J, Arnold R, Rattei T. Gepard: a rapid and sensitive tool for creating dotplots on genome scale. *Bioinformatics.* 2007;**23**: 1026–8
70. McKenna A, Hanna M, Banks E. et al. The genome analysis toolkit: a MapReduce framework for analyzing next-generation DNA sequencing data. *Genome Res.* 2010;**20**: 1297–303
71. Chang CC, Chow CC, Tellier LC. et al. Second-generation PLINK: rising to the challenge of larger and richer datasets. *Gigascience.* 2015;**4**:7
72. Canaguier A, Grimplet J, di Gaspero G. et al. A new version of the grapevine reference genome assembly (12X.v2) and of its annotation (VCost.v3). *Genom Data.* 2017;**14**:56–62
73. Patro R, Duggal G, Love MI. et al. Salmon provides fast and bias-aware quantification of transcript expression. *Nat Methods.* 2017;**14**:417–9
74. Elshire RJ, Glaubitz JC, Sun Q. et al. A robust, simple genotyping-by-sequencing (GBS) approach for high diversity species. *PLoS One.* 2011;**6**:e19379
75. Rastas P. Lep-MAP3: robust linkage mapping even for low-coverage whole genome sequencing data. *Bioinformatics.* 2017;**33**: 3726–32
76. Broman KW, Wu H, Sen S. et al. R/QTL: QTL mapping in experimental crosses. *Bioinformatics.* 2003;**19**:889–90